ISSN 1674-1056
http://cpb.iphy.ac.cn
http://iopscience.iop.org/cpb
中国物理 B
Chinese Physics
中国物理 Chinese Physics B

Superconducting membrane mechanical oscillator based on vacuum-gap capacitor

Yong-Chao Li(李永超), Xin Dai(戴欣), Jun-Liang Jiang(江俊良), Jia-Zheng Pan(潘佳政), Xin-Yu Wei(魏兴雨), Ya-Peng Lu(卢亚鹏), Sheng Lu(卢盛), Xue-Cou Tu(涂学凑), Guo-Zhu Sun(孙国柱), Pei-Heng Wu(吴培亨)
Citation: Chin. Phys. B . 2018, 27(6): 060701. **doi:** 10.1088/1674-1056/27/6/060701

Journal homepage: http://cpb.iphy.ac.cn; http://iopscience.iop.org/cpb

What follows is a list of articles you may be interested in

Compact superconducting single-and dual-band filter design using multimode stepped-impedance resonator

Xiang Wang(王翔), Bin Wei(魏斌), Xi-Long Lu(陆喜龙), Xu-Bo Guo(郭旭波), Bi-Song Cao(曹必松)
Chin. Phys. B . 2017, 26(12): 128501. **doi:** 10.1088/1674-1056/26/12/128501

Superconducting tunable filter with constant bandwidth using coplanar waveguide resonators

Ying Jiang(蒋莹), Bo Li(李博), Bin Wei(魏斌), Xu-Bo Guo(郭旭波), Bi-Song Cao(曹必松), Li-Nan Jiang(姜立楠)
Chin. Phys. B . 2017, 26(10): 108501. **doi:** 10.1088/1674-1056/26/10/108501

High-temperature superconducting filter using self-embedding asymmetric stepped impedance resonator with wide stopband performance and miniaturized size

Dan Wang(王丹), Bin Wei(魏斌), Yong Heng(衡勇), Bi-Song Cao(曹必松)
Chin. Phys. B . 2017, 26(10): 108502. **doi:** 10.1088/1674-1056/26/10/108502

Design and characterization of a 3D encapsulation with silicon vias for radio frequency micro-electromechanical system resonator

Ji-Cong Zhao(赵继聪), Quan Yuan(袁泉), Feng-Xiang Wang(王凤祥), Xiao Kan(阚骁), Guo-Wei Han(韩国威), Ling Sun(孙玲), Hai-Yan Sun(孙海燕), Jin-Ling Yang(杨晋玲), Fu-Hua Yang(杨富华)
Chin. Phys. B . 2017, 26(6): 060705. **doi:** 10.1088/1674-1056/26/6/060705

Improvement of fabrication and characterization methods for micromechanical disk resonators

Zhao Hui, Luo Wei, Zheng Hai-Yang, Yang Jin-Ling, Yang Fu-Hua
Chin. Phys. B . 2012, 21(10): 100702. **doi:** 10.1088/1674-1056/21/10/100702

Superconducting membrane mechanical oscillator based on vacuum-gap capacitor*

Yong-Chao Li(李永超)[1,2,†], Xin Dai(戴欣)[1,2,†], Jun-Liang Jiang(江俊良)[1,2,†], Jia-Zheng Pan(潘佳政)[1,2], Xing-Yu Wei(魏兴雨)[1,2], Ya-Peng Lu(卢亚鹏)[1,2], Sheng Lu(卢盛)[1,2], Xue-Cou Tu(涂学凑)[1,2], Guo-Zhu Sun(孙国柱)[1,2,‡], and Pei-Heng Wu(吴培亨)[1,2]

[1] *Research Institute of Superconductor Electronics, School of Electronic Science and Engineering, Nanjing University, Nanjing* 210093, *China*
[2] *Synergetic Innovation Center of Quantum Information and Quantum Physics, University of Science and Technology of China, Hefei* 230026, *China*

(Received 16 January 2018; revised manuscript received 29 March 2018; published online 10 May 2018)

Using the diluted S1813 UV photoresist as a sacrificial layer, we successfully fabricate a superconducting suspended parallel-plate capacitor, in which the top layer of aluminum film acts as a membrane mechanical resonator. Together with a superconducting octagonal spiral inductor, this parallel-plate capacitor constitutes a superconducting microwave resonator. At mK temperature, the transmission characteristic and spectrum of the microwave resonator are measured. Sideband frequencies caused by the vibration of the membrane mechanical resonator are clearly demonstrated. By down-converting with a mixer, the dependence of fundamental frequency and its harmonics on the input microwave power are clearly demonstrated, which is consistent with the numerical simulation.

Keywords: superconducting membrane mechanical oscillator, vacuum-gap capacitor

PACS: 07.10.Cm, 81.07.Oj, 85.25.–j, 85.85.+j **DOI:** 10.1088/1674-1056/27/6/060701

1. Introduction

Recently, considerable attention has been paid to the research of mechanical resonators, and their classical[1–4] and quantum[5,6] characteristics. Due to its low loss, superconductor material has been used to fabricate mechanical resonators.[7–9] Though interesting quantum phenomena have been explored in such superconducting mechanical resonators, detailed exploration of their classical characteristics is lacking. Instead of solid material we choose the diluted S1813 photoresist as a sacrificial layer, which can be easily removed by acetone, and successfully fabricate a parallel-plate capacitor, in which the suspended top layer film acts as a membrane resonator. Because the device is measured in a vacuum, such a capacitor is usually named a vacuum-gap capacitor (VGC).[10] Note that the structure here is quite different from that in previous work,[11] in which the top layer film of VGC is fixed due to the posts used to support the top plate. Thus the vibration of top layer film is suppressed. Another difference is the method to stimulate the vibration of the mechanical resonator. Usually an electrostatic bias is used in previous work. Here the VGC together with a superconducting octagonal spiral inductor constitutes a superconducting microwave resonator, which is coupled to a coplanar waveguide transmission line. A microwave signal is used to measure the characteristics of the device and at the same time to stimulate the vibration of the membrane mechanical resonator. The vibration of the top layer membrane changes the distance of the gap in the capacitor and thus modulates the frequency of the microwave resonator, the characteristics of which can be detected with a network and a spectrum analyzer.

2. Device fabrication

Our device is composed of an octagonal spiral inductor L and a parallel-plate capacitor C. Figure 1(a) shows the optical photograph of the LC resonator. The insets show the SEM of the corner part of VGC and the overlapping part of the inductance layer and the lower layer of VGC, from which the suspended structures are clearly demonstrated. Such an LC resonator is coupled to a coplanar waveguide transmission line, which is used to measure the resonant characteristics of the LC circuit. The value of the inductor is simulated with FastHenry. The capacitor here has a suspended structure and its value significantly depends on the area of the parallel-plate and the distance between the plates, which can be determined by the parallel-plate capacitor formula.

Figure 1(b) shows the detailed fabrication procedure as follows.

(i) A 50-nm-thick aluminum film was deposited by electron beam evaporation on a high-resistivity silicon substrate and the lower electrode plate of VGC was fabricated by the

*Project supported by the National Key Research and Development Program of China (Grant No. 2016YFA0301801), the National Natural Science Foundation of China (Grant Nos. 11474154 and 61521001), and the Priority Academic Development Program of Jiangsu Higher Education Institutions and Dengfeng Project B of Nanjing University, China.

†These authors contributed equally to this work.
‡Corresponding author. E-mail: gzsun@nju.edu.cn

lift-off process.

(ii) The diluted S1813 with a certain thickness is used to form a sacrificial layer, which was then patterned through UV photolithography.

(iii) Another aluminum film was deposited to form the rest of the circuit, including the top electrode plate of VGC, the octagonal spiral inductor and the coplanar waveguide transmission line by wet etching. Note that the sacrificial layer is completely covered except the four corners by the top capacitor plate after wet etching of aluminum. This is extremely important for removing the sacrificial layer with acetone in the final step.

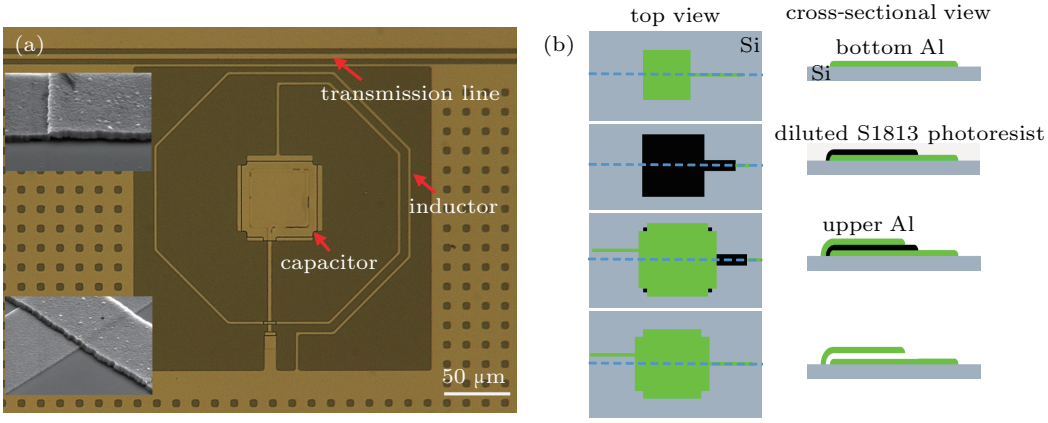

Fig. 1. (color online) (a) Optical photograph of *LC* resonator coupled to a coplanar waveguide transmission line. The upper and lower insets show SEM images of the corner part of VGC and the overlapping part of the inductor and the lower electrode of VGC, respectively. (b) Fabrication procedure for VGC. Top view and cross-sectional view along the dashed line in the top view are presented, respectively.

3. Measurement and analysis

A schematic diagram of our measuring circuit is shown in Fig. 2. At room temperature, the input microwave signal is divided into two parts by a splitter. One of them was fed into the cryostat and the other one was used as the local signal of a mixer, which was used as a down-converter of the amplified output microwave signal from the device. A network analyzer was used to measure the transmission characteristic and a spectrum analyzer was used to characterize the noise spectrum of the device. A computer was used to automatically record the data from the microwave source, network analyzer and spectrum analyzer. Our device was located in a dilution refrigerator with a base temperature lower than 20 mK. The detailed description of the measuring circuits in the cryostat has been given in Ref. [12].

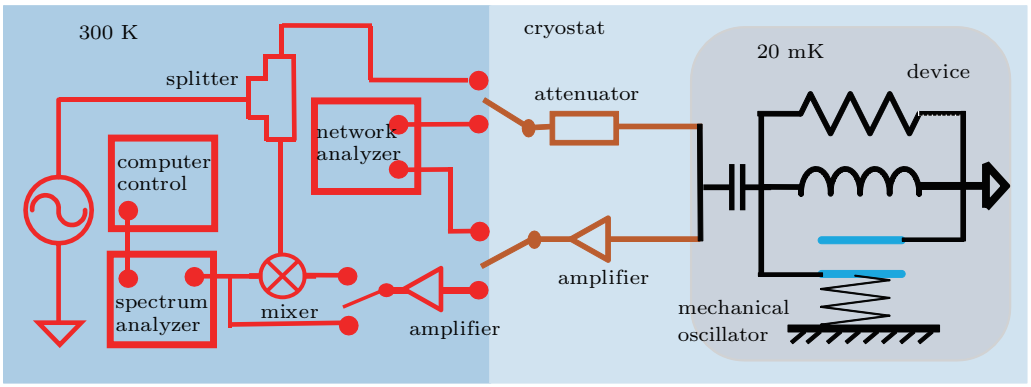

Fig. 2. (color online) Measurement set-up for testing the transmission characteristic and down-converted sideband frequency of the device.

Figure 3 shows the transmission characteristic S_{21} obtained with a vector network analyzer, in which a resonance dip appears as expected. This resonance dip comes from the coupling of the superconducting *LC* microwave circuit to the transmission line. Due to the structure of the resonator, we used $f = 1/2\pi\sqrt{LC}$ to determine the resonant frequency, in which the inductance of the resonator was calculated by FastHenry and the parallel-plate capacitor was determined from $C = S \cdot \varepsilon_0/d$ with $S = 45\ \mu\text{m} \times 45\ \mu\text{m}$ area. Here ε_0 is the permittivity of a vacuum and d is the distance between the top and lower plates. With $L = 1.399$ nH and $f = 5.778$ GHz, we obtained an actual capacitance value of 0.54 pF of VGC and a distance of 33 nm between the capacitor plates.

After knowing the resonant frequency of the superconducting microwave *LC* circuit, we measure the spectrum to obtain the effect of the mechanical resonator on the microwave

resonator. As shown in Fig. 2, a microwave signal with the resonant frequency 5.788 GHz is applied to the device. A spectrum analyzer is used to obtain the spectrum. As is well known, when the frequency of the microwave source is equal to the resonant frequency of the microwave *LC* circuit, most of the input power will be coupled into the *LC* circuit. When the electric field energy stored in the VGC reaches a certain threshold, the electric force will trigger the vibration of the top layer of aluminum film. Such an electromechanical coupling together with mechanical motion results in the frequency conversion of the input microwave. As we can see from Fig. 4(a), when the nominal power of the microwave signal is −19 dBm, only one peak, which is corresponding to the resonance dip in S_{21}, occurs. As the power increases to −18 dBm, four more peaks appear. These peaks are located at regular intervals on both sides of the resonant peak. We gradually increase the microwave power and extract the position of the peaks from the measured spectrum. As shown in Fig. 4(b), with increasing power, the resonant peak remains unchanged while the sideband peaks move further away from the resonant peak.

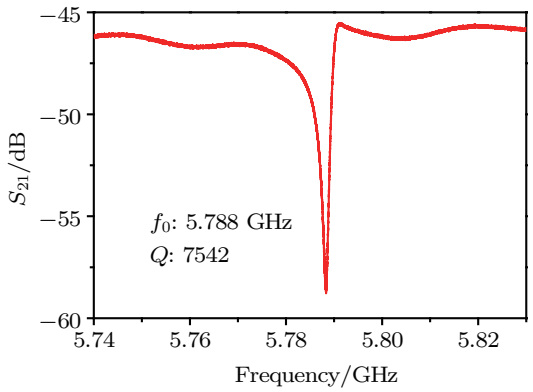

Fig. 3. (color online) Plot of measured S_{21} versus frequency of the transmission line, where a resonance dip is due to the coupling of the superconducting microwave resonant circuit to the transmission line. The resonant frequency and quality factor are 5.788 GHz and 7542, respectively.

Homodyne technology is used to down-convert the microwave frequency. As shown in Fig. 5(a), several peaks are distributed equally, corresponding to the blue sideband frequencies in Fig. 4(b). Note that the lowest frequency is the fundamental frequency of the membrane mechanical resonator. The higher frequencies do not correspond to the high-order vibration modes of the mechanical resonator but the harmonics of the mechanical fundamental frequency. These harmonics are caused by the nonlinear transfer characteristic of the microwave resonator system.[13] Again, by increasing the microwave power, the fundamental frequency and its harmonics will change. Figure 5(b) shows the extracted position of the fundamental frequency and its harmonics versus the nominal microwave power, which are fitted by parabolic functions as indicated by the solid lines. These are consistent with previous results,[3] in which a static gate voltage is used to modify the resonant frequency of the mechanical resonator. Here when a microwave signal is used, the induced instant electric attractive force[1,14] will draw the top layer of VGC downward and produce a tension, which is related directly to the stiffness of the vibrator. This tension is proportional to the square of the instant electric force thus the nominal power of the applied microwave signal. On the other hand, the shift of the fundamental frequency is proportional to the square root of the tension.[15] So there is a parabolic relationship between the nominal applied power and the fundamental frequency.

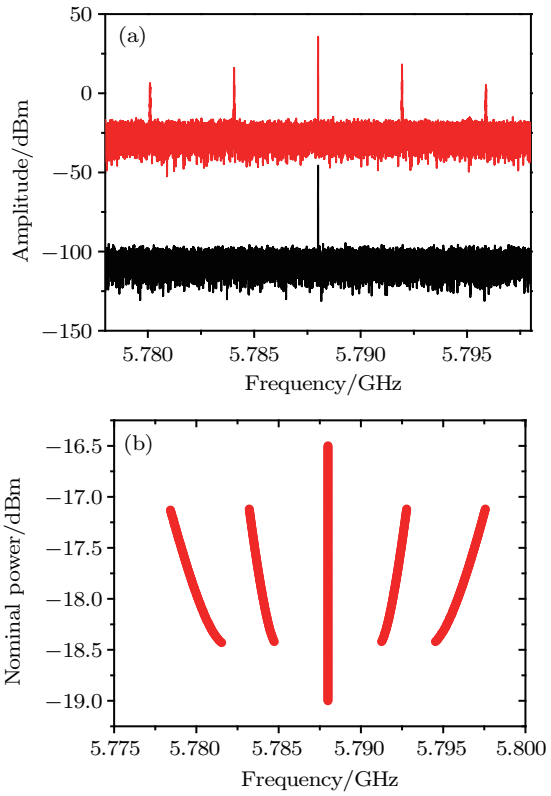

Fig. 4. (color online) (a) Spectrum measured at different input microwave powers. When the input power is −19 dBm, there is only one peak (lower). When the input power increases to −18 dBm, four sideband frequencies appear (upper). (b) Positions of peaks versus the nominal input microwave power.

In order to confirm the experimental results of our superconducting membrane mechanical resonator, we numerically simulate the vibration behavior of the suspended structure, by scanning the parameters of the pretension. As shown in Fig. 6, we find that the dependence of the pretension on the fundamental frequency of the vibrator also satisfies a parabolic function. Note that the simulated fundamental frequency without pretension in our device is 0.82 MHz, while the lowest one in the measured fundamental frequencies is about 3.35 MHz. Their difference may come from two reasons: one is that in the fabrication process of the device, the photoresist is baked at 115 Centigrade, which is equivalent to an annealing treatment of the device, thereby increasing the pretension of the suspended membrane and thus the mechanical vibration

frequency;[16,17] the other possible reason is that there is no static gate voltage to activate the mechanical resonator in our system. When the equivalent electric force induced by the input microwave power is less than a certain threshold, there is no obvious vibration which can be measured. Thus the lowest one in the measured fundamental frequencies is higher than the simulated one without pretension.

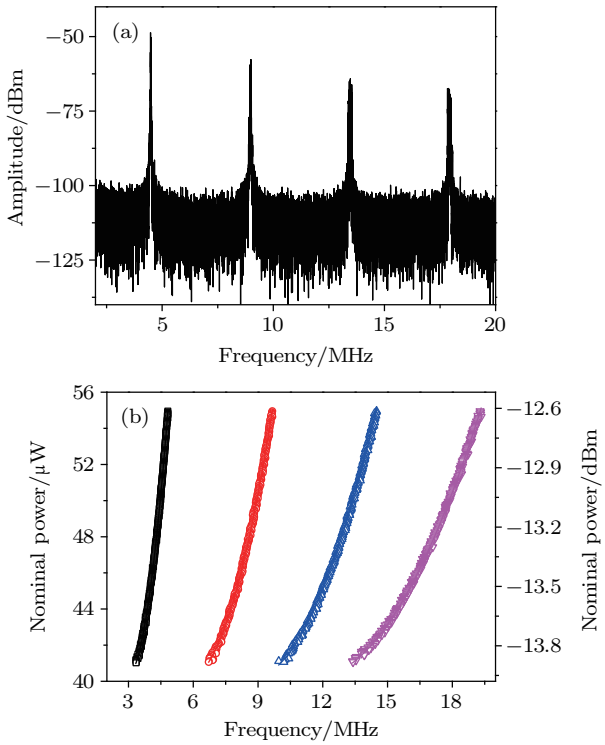

Fig. 5. (color online) (a) Blue sideband frequencies down-converted by a mixer. Nominal input power is −13 dBm. (b) Fundamental frequency and its harmonics of the mechanical resonator. Parabolic relations between input power and resonant frequency are clearly demonstrated. Experimental and fitting data are indicated by symbols and solid lines, respectively.

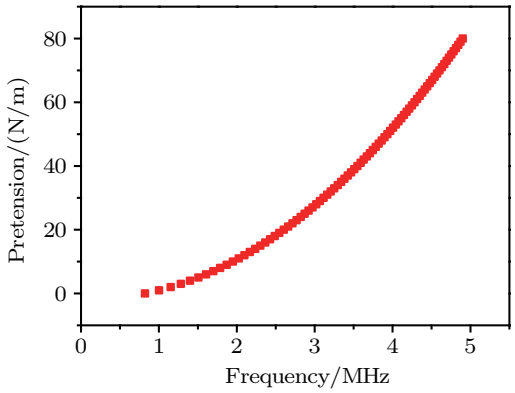

Fig. 6. (color online) Simulated relationship between pretension and fundamental frequency of the membrane mechanical resonator.

4. Conclusions

Using the diluted S1813 photoresist as a sacrificial layer instead of solid material, which needs a long reactive ion etching procedure, we have successfully fabricated a membrane mechanical resonator in a vacuum-gap capacitor. The fundamental vibration frequency and its harmonics of the mechanical resonator are measured through an *LC* microwave resonator. The input microwave power has a parabolic dependence on the fundamental vibration frequency, which accords well with the numerical simulation. Such devices promise to serve as a medium between microwave and mechanical signals and/or even optical signals. What is more, they can also be used to explore quantum behavior of the mechanical vibration, which is important for quantum information processing.

References

[1] Xu Y H, Chen C Y, Deshpande V V, DiRenno F A, Gondarenko A, Heinz D B, Liu S M, Kim P and Hone J 2010 *Appl. Phys. Lett.* **97** 243111

[2] Kozinsky I, Postma H W C, Bargatin I and Roukes M L 2006 *Appl. Phys. Lett.* **88** 253101

[3] Bannon F D, Clark J R and Nguyen C T C 2000 *IEEE Journal of Solid-State Circuits* **35** 512

[4] DeMartini B E, Rhoads J F, Turner K L, Shaw S W and Moehlis J 2007 *Journal of Microelectromechanical Systems* **16** 310

[5] LaHaye M D, Buu O, Camarota B and Schwab K C 2004 *Science* **304** 74

[6] Chan J, Mayer Alegre T P, Safavi-Naeini A H, Hill J T, Krause A, Groeblacher S, Aspelmeyer M and Painter O 2011 *Nature* **478** 89

[7] Wollman E E, Lei C U, Weinstein A J, Suh J, Kronwald A, Marquardt F, Clerk A A and Schwab K C 2015 *Science* **349** 952

[8] Teufel J D, Li D, Allman M S, Cicak K, Sirois A J, Whittaker J D and Simmonds R W 2011 *Nature* **471** 204

[9] Teufel J D, Donner T, Li D, Harlow J W, Allman M S, Cicak K, Sirois A J, Whittaker J D, Lehnert K W and Simmonds R W 2011 *Nature* **475** 359

[10] Cicak K, Allman M S, Strong J A, Osborn K D and Simmonds R W 2009 *IEEE Trans. Appl. Supercond.* **19** 948

[11] Cicak K, Li D, Strong J A, Allman M S, AltomareF, Sirois A J, Whittaker J D, Teufel J D, Simmonds R W 2010 *Appl. Phys. Lett.* **96** 093502

[12] Pan J Z, Cao Z M, Fan Y Y, Zhou Y, Lan D, Liu Y H, Chen Z P, Li Y C, Cao C H, Xu W W, Kang L, Chen J, Yu H F, Yu Y, Sun G Z, Wu P H 2015 *Chin. Phys. B* **24** 110301

[13] Rokhsari H, Kippenberg T J, Carmon T, Vahala K J 2005 *Opt. Express* **13** 5293

[14] Sapmaz S, Blanter Y M, Gurevich L and Zant H S J 2003 *Phys. Rev. B* **67** 235414

[15] Sazonova V, Yaish Y, Üstünel H, Roundy D, Arias T A and McEuen P L 2004 *Nature* **431** 284

[16] Solanki H S, Sengupta S, Dhara S, Singh V, Patil S, Dhall R, Parpia J, Bhattacharya A and Deshmukh M M 2010 *Phys. Rev. B* **81** 115459

[17] Regal C A, Teufel J D and Lehnert K W 2008 *Nat. Phys.* **4** 555